

# Learning Unseen Emotions from Gestures via Semantically-Conditioned Zero-Shot Perception with Adversarial Autoencoders

Abhishek Banerjee, Uttaran Bhattacharya, Aniket Bera

Department of Computer Science, University of Maryland  
College Park, Maryland 20740, USA  
{abanerj8, uttaranb, bera}@umd.edu  
<https://youtu.be/yalthVwTJ5s>

## Abstract

We present a novel generalized zero-shot algorithm to recognize perceived emotions from gestures. Our task is to map gestures to novel emotion categories not encountered in training. We introduce an adversarial, autoencoder-based representation learning that correlates 3D motion-captured gesture sequence with the vectorized representation of the natural-language perceived emotion terms using *word2vec* embeddings. The language-semantic embedding provides a representation of the emotion label space, and we leverage this underlying distribution to map the gesture-sequences to the appropriate categorical emotion labels. We train our method using a combination of gestures annotated with known emotion terms and gestures not annotated with any emotions. We evaluate our method on the MPI Emotional Body Expressions Database (EBEDB) and obtain an accuracy of 58.43%. This improves the performance of current state-of-the-art algorithms for generalized zero-shot learning by 25–27% on the absolute.

## 1 Introduction

Emotion recognition as an area of research is integral to a variety of domains, including human-computer interaction, robotics (Liu et al. 2017), surveillance (Arunnehr and Geetha 2017) and affective computing (Yates et al. 2017). Existing research in emotion recognition has leveraged aspects such as facial expressions (Liu et al. 2017), speech (Tawari and Trivedi 2010), biometric sensing (Zhao, Adib, and Katabi 2016) and gaits (Bhattacharya et al. 2020) to gauge an individuals emotional state. Gestures have also been used in psychological studies to identify emotions, by using affective features such as arm swing rate, posture, frequency of movements, etc (Michalak et al. 2009), (Meeren, van Heijnsbergen, and de Gelder 2005). Recent work by (Bhattacharya et al. 2020) has leveraged spatial-temporal graph convolution networks (ST-GCN) (Yan, Xiong, and Lin 2018) to capture pose dynamics and generate a mapping between the extracted features and the labeled emotions.

A major challenge in machine learning-based emotion recognition algorithms is the requirement for significantly-sized, well-labeled datasets to build classification algorithms on previously labeled emotions. However, considering the wide spectrum of emotions for humans (Zhou et al. 2016) and different emotion representations (Ekman and Friesen

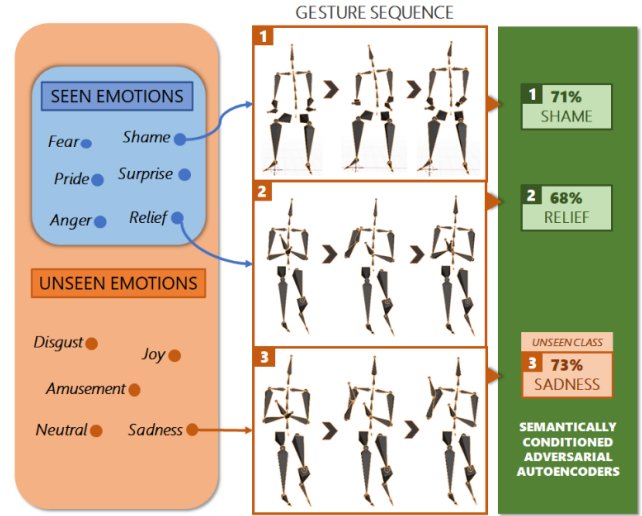


Figure 1: **Generalized zero-shot Emotion Recognition from gestures.** Gesture sequences from both seen and unseen classes of emotions are used as the input to our AAE-based representation learning algorithm. We capture the spatial-temporal representation of 3D motion-captured gesture sequences in our network and correlate them with the semantic representation of the corresponding perceived emotion term. Our network can accurately recognize emotions not seen during training and has an overall accuracy of 58.43%.

1967), it is tedious and often prohibitively expensive to develop datasets with an adequate number of instances for every emotion. Zero-shot learning has recently drawn considerable attention to overcome such issues where labels of different classes are unavailable. It provides an alternative methodology that does not rely on existing labels. Instead, it relies on utilizing the different relationships between various seen and unseen classes to determine the appropriate labels.

In the generalized zero-shot learning (GZSL) paradigm, a network learns to recognize all classes, seen and unseen, while being trained with data annotations available only for seen classes. The model learns to generalize on the unseen classes by leveraging information from other modalities, such as language semantics, to create class embeddings corresponding to each label. Recent approaches to the zero-shot

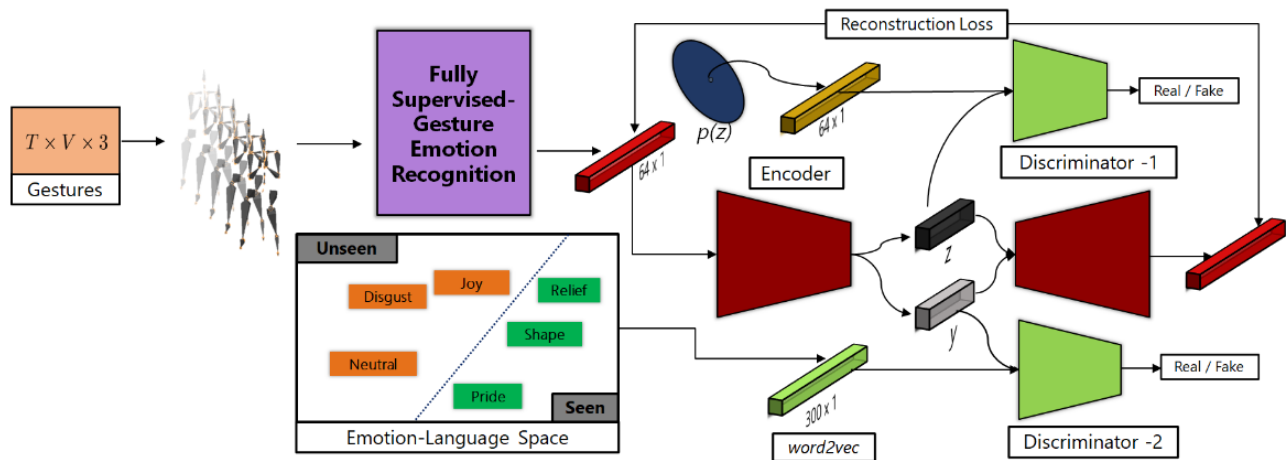


Figure 2: **Network overview.** Our network consists of a feature extraction pipeline that takes the sequence of gestures ( $T$ : time steps,  $V$ : joints or nodes) and extracts the relevant high-level features. These features are fed into a semantically-conditioned adversarial autoencoder, which projects these features onto a latent space by aligning it with the word-level semantic information from the word2vec dimension. The network’s encoder generates two latent vectors, corresponding to the embeddings for the gestures and the word embeddings. The adversarial loss is used by the two discriminators to align the latent distributions to the corresponding priors.

problem have used generative models (Mishra et al. 2018; Chen et al. 2018; Long et al. 2017) to synthesize features for the unseen classes, which are then used for the classification task. GANs and VAEs have been the most prominent methods to synthesize these features; however, Shi et al. (Shi et al. 2019) have shown that the representation of multi-modal distributions by VAEs can result in sub-optimally learned representations. While GANs can create higher quality features than VAEs, the latent distribution spaces they learn can be susceptible to mode collapse (Goodfellow et al. 2014). On the other hand, adversarial autoencoders (AAEs) create more closely aligned latent distributions than VAEs or GANs (Makhzani et al. 2015). Therefore, we build on the network by Makhzani et al. (Makhzani et al. 2015) to develop our network architecture.

**Main Results:** We present a generalized zero-shot algorithm to recognize perceived emotions from 3D motion-captured gesture sequences represented as upper-body poses. To capture the semantic relationships between the emotion classes, we leverage the rich word embeddings of the pre-trained word2vec model (Mikolov et al. 2013). A fully-supervised emotion recognition network generates a feature vector corresponding to a sequence of gesture inputs. We use an autoencoder architecture coupled with an adversarial loss to generate latent representations for the learned gesture-feature vectors learned from the fully supervised network corresponding to gesture sequences, and another adversarial loss to align these latent representations with the semantically conditioned distribution space of the emotion classes. Our main contributions include:

1. A GZSL algorithm, SC-AAE, based on an adversarial autoencoder architecture. We train it to learn a mapping between the gesture-feature vectors corresponding to 3D motion-captured gesture sequences, and the seen and unseen perceived emotion classes expressed in natural lan-

guage. To the best of our knowledge, our method is among the first to classify unseen perceptual affective labels in a zero-shot learning fashion.

2. A fully supervised emotion recognition algorithm, FS-GER that classifies 3D motion-captured gesture sequences seen emotion classes. We use this architecture to generate the feature vectors for input to our SC-AAE for GZSL.

Our fully supervised network achieves a validation accuracy of 77.61% with the seen emotion classes in the MPI Emotional Body Expressions Database (EBEDB) (Volkova et al. 2014), which outperforms state-of-the-art methods for fully supervised action and emotion recognition by 7–18% on the absolute. More importantly, we achieve an accuracy of 58.43% on EBEDB over the collective set 11 seen and unseen emotion classes, outperforming state-of-the-art ZSL methods by 25–27% on the absolute.

## 2 Related Work

We provide an overview of emotion representation, emotion recognition from non-verbal body expressions, and relevant developments in Zero-Shot learning.

### 2.1 Emotion Representation

Inferring emotions from multi-modal cues such as faces, speech, and gestures have been extensively researched in psychology (De Silva et al. 2006; Gunes and Piccardi 2007). There are three primary modeling methods used to analyze emotions (Grandjean, Sander, and Scherer 2008): categorical, appraisal-based, and dimensional. The categorical description (Ekman and Friesen 2003) delineates emotions into a small number of distinct categories that can be universally recognized. However, with the wide spectrum of emotional states exhibited by a person in response to their environments, it is difficult to segregate emotions into a few discrete

states. The appraisal-based method (Grandjean, Sander, and Scherer 2008) uses a continuous subjective-evaluation of the subject’s emotional state and its interdependence on the environment. The dimensional description (Russell 1980) decomposes the emotional-state into three components, valence, arousal, and dominance. The advantage of using a dimensional-relation is that it allows for treating emotions, not as disparate entities but inherently related in a continuous space. A crucial distinction needs to be made between perceived and intended emotions. An intended emotion is generally the emotional state that is self-reported by an individual (Robinson and Clore 2002), which is difficult to procure and can also be misleading as people can be unaware of their true emotional states (Barrett et al. 2007).

The perceived emotion relies on the consensus of what is reported by other people observing a subject, which is more straightforward to collect. We use the perceived categorical emotions in our work on account of the widely available datasets with annotated categorical labels for the emotions. However, we attempt to translate the categorical labels into semantically-conditioned continuous space representation using the language-semantic embedding.

## 2.2 Emotion Recognition

Seminal work on emotion identification from gaits was carried out by (Montepare, Goldstein, and Clausen 1987), with more recent works (Sanders et al. 2016) showcasing the correlation between gaits and inherent psychological stress. Methods of (Sapiński et al. 2019; Garcia-Ceja et al. 2019; Hossain and Muhammad 2019) use deep learning methods to identify emotion states from gestures extracted from videos. Studies by (Wegrzyn et al. 2017) identified people’s emotional states through psychological studies of human facial expressions. Studies by (Cordaro et al. 2016) used vocal cues to determine emotions. With the advent of deep learning, various works have emerged that use vision-based methods (Saragih, Lucey, and Cohn 2009; Akputu, Seng, and Lee 2013) to determine emotional state from facial expressions or audio signals using speech (Deng et al. 2017). Recently, a number of works have used multiple modalities, including speech and facial expressions, in determining emotions (Mittal et al. 2020; Albanie et al. 2018).

Learning emotions from poses involve an inter-relation between various research domains. The method of (Bhattacharya et al. 2020) has used spatial-temporal gait extraction to map the movements to emotions. Other methods have used PCA and SVM based classifiers on affective features (Karg, Kühnlenz, and Buss 2010; Crenn et al. 2016). Despite all the progress, recent studies (Cowen et al. 2019) have shown that the taxonomy of emotions is varied and complex, making it cumbersome to recognize and classify emotions explicitly. This further makes it difficult for deep learning-based methods to recognize and generalize emotions due to the obscurity involved in labeling significantly large datasets with the appropriate emotions.

## 2.3 Generalized Zero-Shot Learning

In the Generalized Zero-Shot Learning (GSZL) problem, the recognition task is executed for both seen and unseen classes. In contrast, for Zero-Shot Learning (ZSL), recognition is attempted on only the unseen classes alone. The

GZSL is more challenging than the nominal-ZSL, where the model classifies only unseen classes because of the hubness problem (Dinu, Lazaridou, and Baroni 2014), which occurs when the model overfits to the trained classes. Recently, generative methods have become popular in GZSL, which uses either GANs (Mishra et al. 2018) or VAEs (Schonfeld et al. 2019) to generate features for unseen classes. Traditional GZSL generative models rely on a data augmentation method, which generates features of interest that have been hitherto unseen by the model during training. Hubert et al. (Hubert Tsai, Huang, and Salakhutdinov 2017) have shown that mapping the joint visual-language features to a latent space instead of the language space gives higher accuracy. It is necessary to reconstruct data across domains by cross-aligning the distributions to get an appropriate mapping for such cases. Schonfeld et al. (Schonfeld et al. 2019) use unconditional VAEs and achieve multi-modal alignment via cross-reconstruction and distribution alignment. In our algorithm, we build on the network model used by (Schonfeld et al. 2019) to perform our latent space embedding and classification task. Considering the multiple modalities that are used to learn the distribution in our approach, *i.e.*, language semantics for emotions and gestures, we rely on methods that correlate the learned distributions of these modalities to estimate the semantic relation between the classes accurately.

## 2.4 Zero Shot Action Recognition

To the best of our knowledge, recognition of emotions from gestures has not been previously explored in the zero-shot paradigm. However, a closely related domain is that of action recognition. Methods on zero-shot learning have addressed action recognition given videos or motion capture sequences. Methods in this domain mainly use language or word-based semantic relation between the classes to classify actions by projecting extracted visual features onto the language space. Recent work in this field has used methods ranging from error correction codes (Qin et al. 2017), GANs (Zhu et al. 2018), as well as relational networks that explore a 3D-pose sequence-based nearest neighbor classification to determine specific actions. In (Gao, Zhang, and Xu 2019), the authors build knowledge graphs to learn relationships between action class labels and two-stream networks to learn visual features from the image frame. Our work relies on the features extracted from a sequence of 3D poses to determine the class.

## 3 Method

In this section, we define the problem statement and describe our approach in detail. We present an overview of our proposed algorithm in Figure 2. We use the sequence of 3D motion-captured poses as input to our pre-trained feature extraction module to obtain the corresponding feature vectors. Subsequently, using the *word2vec* representation, we obtain the semantic word-level embedding for the specific emotion. The semantic embedding and the corresponding feature vector are used as inputs to the SC-AAE architecture. The encoder part of the VAE outputs a class semantic label as well as a latent vector. The two vectors are passed through two subsequent discriminators that use the adversarial loss to increase the encoder’s estimated classification accuracy. For

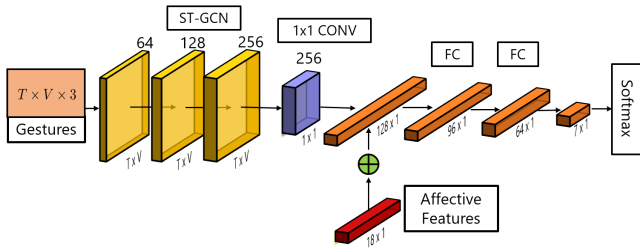


Figure 3: **Fully Supervised Network for Emotion Recognition from Gestures (FS-GER)**. The network comprises of three ST-GCN layers, followed by a single  $1 \times 1$  convolution layer. The input data is of the form  $T$ : time Steps (510 at 30fps)  $\times V$ : nodes (10 joints)  $\times 3$  (dimension of nodes). The convolution output is appended with the affective features,  $A$ , and then passed through subsequent Fully Connected (FC) layers to generate a 64-dimensional feature description vector. This layer is passed through an FC of size 7 (total number of classes on which it is trained). The softmax layer uses this for classification. The 64-dimensional embedding is extracted from the network after the fully supervised step for the GZSL task.

classification, we use the encoder to output the corresponding semantic labels, which are then matched with the relevant class labels.

### 3.1 Problem Definition

We discuss the task definition of our approach in this section. Let  $S = \{(x, y, c(y)) \mid x \in X, y \in Y^S, c(y) \in C\}$  be a set of input data. Here  $x$  denotes an input vector embedding representing a sequence of gestures, and  $y$  is the corresponding class label, which in our approach is the associated emotion.  $c(y)$  is the semantic embedding corresponding to the class label. In our work, we use the *word2vec* representation for the semantic description (described later in Section 3.3). We also have the auxiliary training set  $U = \{(u, c(u)) \mid u \in Y^U, c(u) \in C\}$ , for all the unseen classes. Here,  $u$  denotes an unseen class from the set  $Y^U$ , which is disjoint from  $Y^S$ . The task that we have at hand is the GZSL task, which evaluates the network on both seen and unseen classes, denoted by  $f_{GZSL} : X \rightarrow Y^S \cup Y^U$ .

We approach our problem of GZSL in the transductive setting (Wan et al. 2019). In the transductive setting, the pre-trained network has access to the unseen classes, but the data points in these classes do not have any associated labels. We create a single dummy label for all the gestures belonging to all the unseen classes during feature generation using the pre-trained network. We first start with a description of the feature generation module, which generates an embedding corresponding to the input sequence of gestures.

### 3.2 Feature Extractor Network

We show an overview of the feature extraction network in Figure 3. The input to the network is a sequence of poses of size  $T$  (time steps)  $\times V$  (nodes)  $\times 3$  (position coordinates). Because gestures are a periodic sequence of poses, we use ST-GCN (Yan, Xiong, and Lin 2018), which captures spatial and temporal features of interest for the input gaits. The

Table 1: **Affective Features**. We extract the motion and posture features from an input gait using emotion characterization in visual perception and psychology literature

Features	Description
<i>Volume</i>	Bounding Box
<i>Angle</i>	With shoulders at neck With neck and left shoulder at right shoulder With neck and right shoulder at left shoulder With vertical-direction and back at neck With head and back at neck
<i>Distance</i>	Between right wrist and root joint Between left wrist and root joint
<i>Area</i>	Triangle between neck and wrists
<i>Speed</i>	Of left wrist Of right wrist Of head
<i>Acceleration</i>	Of left wrist Of right wrist Of head
<i>Jerk</i>	Of left wrist Of right wrist Of head

relationship between specific joints is defined using an adjacency matrix, and this relationship is leveraged while using the GCNs. The first ST-GCN layer has 64-layers while the second and third have 128 and 256-layers, respectively. ST-GCN layers are followed by a ReLU activation function and a BatchNorm layer. The output of the convolution operation is passed through a  $1 \times 1$  convolution layer, giving a 128-dimensional vector. This is appended with an affective feature vector extracted from the gestures during pre-processing and is subsequently passed through two successive fully connected (FC) layers, to give a  $64 \times 1$  feature vector. This feature vector is passed through a fully connected layer, followed by a softmax layer to generate labels for classification. We treat the feature vectors belonging to unseen classes,  $Y^U$  as a single class with a dummy label.

The gestures are predominantly in the upper part of the body; therefore, we consider only the relevant joints in the upper body. Affective features from gestures have been shown to be relevant to the problem of emotion recognition (Randhavane et al. 2019; Bhattacharya et al. 2020), and consist of posture and motion features:

- **Posture features**: These consist of distances between pairs of joints, as well as angles and areas formed by three joints of interest.
- **Motion features**: These consist of velocity and acceleration of joints of interest in the gesture.

Based on visual perception and psychology literature (Karg, Kühnlenz, and Buss 2010; Crenn et al. 2016), we use 18 extracted features, denoted by  $A$ , which we append to the output of the ST-GCN layers. We list these features in Table 1.

### 3.3 Language Embedding

The key idea in our zero-shot learning is to utilize the semantic relationship between multiple classes of emotions to determine the association between various gesture sequences and the seen and unseen emotion classes. The *word2vec* (Mikolov et al. 2013) representation gives a 300-dimensional embedding vector based on the semantics of the word. Using the vector representations for all emotions, we can ascertain the level of “closeness” or “disparity” between them. For the unseen classes, these representations give us the underlying relationship between instances of that class and other classes in the seen and unseen domains, allowing us to classify them into the appropriate categories.

We represent the set of emotions as

$$\mathcal{E} = \{e_1, e_2, e_3, \dots, e_n\}, \quad (1)$$

where  $\{e_i\} \in \mathbb{R}^{300}$  is the *word2vec* representation of the emotion-word. This way, two specific emotions can be related by Euclidean  $\ell_2$ -norm distance to ascertain their adjacency.

### 3.4 Variational Autoencoder

Variational autoencoders (VAEs) are generative models based on the principles of Bayesian variational inference and attempt to find the distribution  $p_\phi(x)$ , parametrized by  $\phi$  and given by

$$p_\phi(x) = \int p_\phi(x|z)p(z)dz, \quad (2)$$

where  $z$  represents a variable in the latent space being mapped and is assumed to exhibit a Gaussian prior given by  $p(z)$ . The Gaussian assumption is also held to be true for the conditionals  $p_\phi(x|z)$  and these are modeled by the decoder of the network. VAEs work by approximating  $p_\phi(z|x)$  with factorized distributions  $q_\theta(z|x)$  and they infer parameters  $\phi$  through the encoder part of the network. On account of the general intractability in finding  $p_\phi(z|x)$  given the form of the integral, the VAE uses the ELBO bound to get an approximate solution  $q_\theta(z|x)$ . The objective function becomes

$$\mathcal{L} = \mathbb{E}_{q_\phi(z|x)} [\log p_\theta(x|z)] - D_{KL}(q_\phi(z|x) \| p_\theta(z)). \quad (3)$$

The first term is the reconstruction loss. The second term is the Kullback-Leibler divergence  $D_{KL}$ . The VAE predicts  $\mu$  and  $\Sigma$  such that  $q_\phi(z|x) = \mathcal{N}(\mu, \Sigma)$ .

### 3.5 Generative Adversarial Networks

The Generative Adversarial Network (GAN)(Goodfellow et al. 2014) framework establishes a min-max adversarial game between two neural network components, a generator model  $G(z)$  and a discriminator model  $D(x)$ . The discriminator  $D(x)$  is a neural network that aims to map the real and the generated data points into different distribution spaces. Conversely,  $G(z)$  takes a latent input  $z$  from a prior distribution  $p(z)$  and aims to map it onto the distribution space of real points being learned by the discriminator. As these two networks attempt to optimize their own objectives, the system reaches the Nash Equilibrium(Holt and Roth 2004). The joint objective function can be expressed as

$$\min_G \max_D \mathbb{E}_{\mathbf{x} \sim p_{\text{data}}} [\log D(\mathbf{x})] + \mathbb{E}_{\mathbf{z} \sim p(\mathbf{z})} [\log(1 - D(G(\mathbf{z})))] \quad (4)$$

In our method, we implement two discriminators which use the adversarial loss described above to identify true samples from the underlying distributions for both gestures and language-based semantic distributions.

### 3.6 Adversarial Autoencoder

In our current method, we build on the work of (Makhzani et al. 2015) to create an adversarial autoencoder, which learns from the semantic distributions of data in the language space as well as the gesture space. The VAE in such a setting is regularized by matching the posterior  $q(z|x)$  to a prior  $p(z)$  distribution. The training of the network takes place in two phases:

- the *reconstruction phase*, where the autoencoder updates the encoder and the decoder to minimize the reconstruction error of the inputs, and
- the *regularization phase*, where the adversarial network first updates its discriminative network to separate the true samples from the generated samples. The generator we use to compute the adversarial loss in our case comes from the encoder network of the VAE.

### 3.7 Network Architecture

As seen in Figure 2, FS-GER outputs a 64-dimension feature vector for the respective gesture input sequence. Correspondingly, we get the 300-dimension language embedding using *word2vec*. The encoder for the adversarial autoencoder (AAE) predicts the latent vector corresponding to the gesture  $z$  and the class semantic label,  $\hat{y}$ . The generated labels and vectors are then passed through two separate discriminators that help discriminate between the desired samples from the prior and those generated by the encoder. After the training, we use the encoder to generate the relevant semantic labels, which identifies the predicted emotion label corresponding to that gesture-sequence input.

### 3.8 Loss Functions

We aim to minimize the cross-alignment loss between gestures and the word-labels. As we have two separate modalities, we utilize two separate VAEs akin to those in (Schonfeld et al. 2019) to map the inputs to a common latent space. Thus, based on Equation 3, we can write the loss as

$$\mathcal{L}_{VAE} = \mathbb{E}_{q_\phi(z|x)} [\log p_\theta(x^{(i)}|z)] - \beta D_{KL}(q_\phi(z|x^{(i)}) \| p_\theta(z)). \quad (5)$$

The KL divergence aligns the desired distributions. In our algorithm, we use the adversarial losses to align the prior distributions with the encoder output, hence do not use the KL divergence.

**Adversarial Loss** As per Equation 4, we can write the adversarial loss for a discriminator as

$$\mathcal{L}_{ADV} = \mathbb{E}_{\mathbf{x} \sim p(\mathbf{x})} [\log D(\mathbf{x})] + \mathbb{E}_{\tilde{\mathbf{x}} \sim p_\theta(\tilde{\mathbf{x}}|\mathbf{z}, \mathbf{a})} [\log(1 - D(\tilde{\mathbf{x}}))] \quad (6)$$

There are two adversarial losses used in our network, corresponding to two discriminators. For the label discriminator,  $a$  corresponds to  $c(y)$ , which is an element of  $\mathcal{E}$ , in Equation 1. We denoted this by  $\mathcal{L}_{ADV-label}$ . For the feature discriminator, it corresponds to an element from the generated features from a prior distribution  $p(z)$  and we denote the adversarial loss for this by  $\mathcal{L}_{ADV-feature}$

Hence, we can write our net loss as

$$\mathcal{L}_{NET} = \mathcal{L}_{VAE} + \gamma \mathcal{L}_{ADV-lang} + \delta \mathcal{L}_{ADV-feat}, \quad (7)$$

where  $\gamma$  and  $\delta$  are weighing functions.

## 4 Results and Experiments

We present experiments and results for our zero-shot classification task in this section, including the details of our network and the hardware configuration.

### 4.1 Dataset

We train and evaluate our network on the MPI Emotional Body Expressions Database (EBEDB) (Volkova et al. 2014). It consists of 1,447 3D motion-captured sequences of natural-emotion body gestures from actors as they narrated specific lines. All body movements were captured at 120 fps. The original dataset consists of information regarding 23 joints in the body. However, because we are interested in gestures made by the upper body, we select  $V = 10$  joints: the head, neck, right-shoulder, left-shoulder, right-elbow, left-elbow, right-wrist, left-wrist, backbone, and pelvis. We ignore the lower-body joints as there is no significant motion in those joints. Each sequence is annotated with one of 11 categorical emotion classes.

To evaluate our model, we split the 11 available emotion classes in MPI EBEDB into a roughly equal split of six seen classes and five unseen classes. During the training phase, the model learns only from the six seen classes. Since there are multiple possible combinations for choosing these five unseen classes and there are no fixed criteria in particular for this dataset for zero-shot learning, we conduct five experiments in which we successively select five random classes from the available 11. Our results are averaged over these five experiments. We use a train-test split of 80%-20%.

### 4.2 Training Details

All our encoders and decoders are multi-layer perceptrons with two hidden layers. More hidden layers reduce the performance because the gesture-features and language embeddings are very high-level representations and generally sparse; hence more layers would result in loss of crucial features for classification. We use 100 hidden units each for the encoder and the decoder. The discriminators consist of two hidden layers with 100 hidden layers each for the language-embedding model, while the discriminator for the gesture-feature vector has two hidden layers of size 100 and 32, respectively. In our work, we use the proposed FS-GER to generate a 64-dimension feature vector corresponding to the gestures and a 300-dimension *word2vec* feature encoding the emotions.

We train the model for 200 epochs by stochastic gradient descent using the Adam optimizer (Kingma and Ba 2014) and a batch size of 6 for features. Each batch consists of pairs of extracted gesture features and matching attributes from different seen classes. Pairs of data always belong to the same class. We keep the values of  $\gamma$  and  $\delta$  constant and discuss how we choose their values in Section 4.7. Our network takes around 6 minutes to train on an Nvidia RTX 2080 GPU.

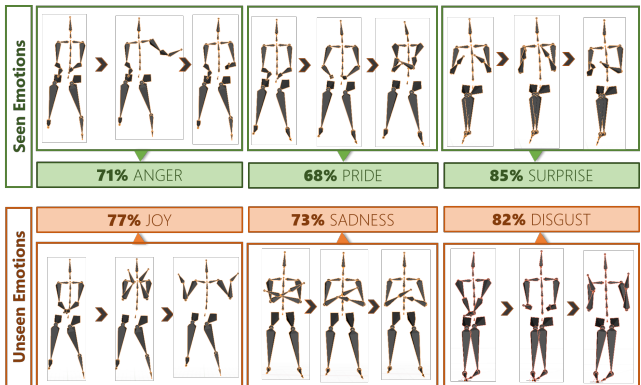


Figure 4: **Visual Results.** The top row shows three sets of gestures in temporal order from left-to-right, which map to the correct seen emotions during classification. The bottom row consists of three gestures mapped to the correct unseen emotions during training.

### 4.3 Performance of FS-GER

We compare the performance of FS-GER (Fully-Supervised Emotion Recognition) with previous methods on emotion recognition (Bhattacharya et al. 2020), as well as action recognition (Yan, Xiong, and Lin 2018). In (Yan, Xiong, and Lin 2018), the authors introduce ST-GCNs to perform action recognition. The network takes a sequence of gaits as input and uses the spatial relation between the various joints and their temporal locations to create a mapping between the motion sequences and their actions. In (Bhattacharya et al. 2020), the authors develop an emotion-specific embedding method to augment the graph convolution network’s ability to map motion patterns to perceived emotions. In addition to capturing the spatial and temporal variance of the joints, they extract certain affective features that capture semantics more specific to emotions. We show the overall network architecture for our network, FS-GER in Fig. 3. We train all networks from scratch using all the body joints as per their input requirements. We classify for the same set of six seen classes and one dummy class corresponding to the five unseen classes. Based on the MPI EBEDB (Volkova et al. 2014), we have  $T = 510$  time steps and  $V = 10$  joints in the upper body.

We report the performance of all the methods in Table 2. We observe that our method outperforms the other methods by 7–18% on the absolute, as a result of using the relevant set of joints and affective features. We use our proposed emotion classifier network to generate features for the subsequent GZSL framework.

Table 2: Classification accuracies for fully-Supervised emotion recognition methods on the seen emotion classes (*colored row is best*).

Method	Accuracy
ST-GCN (Xian et al. 2018)	59.12%
STEP (Schonfeld et al. 2019)	70.38%
<b>FS-GER (Ours)</b>	<b>77.61%</b>

#### 4.4 Related Methods

We compare with ZSL methods for image classification and action recognition. Similar to our method, these methods also attempt to learn mappings from visual as well as spatial-temporal feature vectors to semantic descriptions.

- **Action Recognition.** We compare with (Mandal et al. 2019), which integrates an out-of-distribution task with the generalized action recognition problem. Their method uses a GAN-based feature generation method to generate features for unseen classes. The out-of-distribution detector enabled detection of seen or unseen features to reduce bias towards seen classes.
- **Image Classification.** We compare with state-of-the-art image classification problems in the GZSL paradigm, such as CADA-VAE (Schonfeld et al. 2019), f-CLSWGAN (Xian et al. 2018), and CVAE-ZSL (Mishra et al. 2018). In (Schonfeld et al. 2019), the authors implement two separate VAEs use cross-reconstruction losses to align them. In (Xian et al. 2018), the authors use a GAN-based reconstruction to generate unseen features and leverage the Wasserstein distance to align the multiple-distributions. In (Mishra et al. 2018), the authors implement a standard VAE architecture, and add semantic labels to the inputs for calculating the reconstruction loss. For a fair comparison, we trained all these methods from scratch on MPI EBEDB (Volkova et al. 2014).

#### 4.5 Evaluation Metric

Following previous works in the GZSL paradigm (Schonfeld et al. 2019; Xian et al. 2018), we evaluate performance using the harmonic mean of the accuracies on the seen and the unseen classes. The harmonic mean is given by

$$H = 2 * (acc_{y^{tr}} * acc_{y^{ts}}) / (acc_{y^{tr}} + acc_{y^{ts}}), \quad (8)$$

where  $acc_{y^{tr}}$  and  $acc_{y^{ts}}$  represent the accuracy of gestures from seen and unseen classes, respectively. The harmonic mean is preferred over the more conventional arithmetic mean in this paradigm because the arithmetic mean gives a large value if the seen class accuracy is much greater than the unseen class accuracy. By contrast, the harmonic mean only gives a large value both the seen, and the unseen class accuracies are large, providing a more accurate reflection of performance.

#### 4.6 Evaluation of our Zero-Shot Framework

We evaluate our proposed ZSL approach (SC-AAE) with the other approaches for the GZSL task in Table 3. We report the harmonic mean of the accuracies for the seen and the unseen classes, as achieved by each method. We observe that our proposed approach, SC-AAE, outperforms the other approaches by 25–27% on the absolute. f-CLSWGAN (Xian et al. 2018), which conditioned GANs on image classification, suffers from mode collapse. CADA-VAE (Schonfeld et al. 2019), while aligning the language-semantic and gesture-feature spaces effectively, fails to create representative features for the unseen classes which can help in recognition. CVAE-ZSL (Mishra et al. 2018), which was built for the action recognition task, does not generate robust features for emotion recognition. The visual results for our method can be seen in Figure 4.

Table 3: Harmonic mean of classification accuracies on seen and unseen classes by different methods on our GZSL task (colored row is best).

Method	Harmonic Mean
CADA-VAE (Schonfeld et al. 2019)	33.27%
f-CLSWGAN (Xian et al. 2018)	30.18%
CVAE-ZSL (Mishra et al. 2018)	31.74%
<b>SC-AAE (Ours)</b>	<b>58.43%</b>

#### 4.7 Analysis of the Zero-Shot Model

In this section, we present an analysis of our zero-shot learning architecture, including the choice of hyperparameters and the size of the latent space. For additional analysis and details, please refer to the technical appendix.

**Hyperparameters** Our model uses two hyperparameters,  $\gamma$  and  $\delta$ , for regularizing the loss function for the network. These weigh the effect of the adversarial loss from both discriminators, *i.e.*, from the language embedding and the extracted gait features, on the training process. Fixing  $\gamma$  at 1, we varied  $\delta$  between 0.1 and 2 during training. On account of the heavier usage of the *word2vec* embedding in the determination of classification accuracy, we found  $\delta = 1.5$  to give us the highest harmonic mean of accuracies, and therefore we have used this value to report our results. Changing  $\gamma$  while keeping  $\delta$  fixed at 1.5 did not result in any significant changes, as these changes were largely overshadowed by the gains from changing  $\delta$ . Hence, we set  $\gamma = 1$  for our experiments.

**Size of Latent Embedding** The latent embedding refers to the size of the gesture feature vector used in our latent space. We changed the sizes of the latent embeddings,  $d$ , from  $d = 2$  to  $d = 32$  in steps of one. We obtained the best results for  $d = 16$  and used this in our final network.

## 5 Conclusion, Limitations and Future Work

In this work, we proposed a novel SC-AAE architecture for generalized zero-shot learning of perceived emotions from 3D motion-captured gesture sequences. We used an adversarial loss to learn mappings between the gestures and the semantically-conditioned space of emotion words to classify gestures into both seen and unseen emotions. We evaluated our approach on the MPI Emotional Body Expressions Database (EBEDB), using feature-embeddings extracted from gestures and language-embeddings from *word2vec*. Our proposed approach outperforms previous state-of-the-art algorithms for GZSL by 25–27% on MPI EBEDB.

Our work has some limitations. Since *word2vec* is a generic language-embedding model, not specific to emotions, it may not capture all aspects of psychological and emotional diversity. We, therefore, plan to affective-based semantics from words in the future. We also plan to incorporate more affective modalities, including speech and eye movements, to ensure a more robust classification. Furthermore, we plan to use the dimensional space of VAD (Valence-Arousal-Dominance) to learn relationships between disparate categorical emotions.

## References

- Akputu, K. O.; Seng, K. P.; and Lee, Y. L. 2013. Facial emotion recognition for intelligent tutoring environment. In *2nd International Conference on Machine Learning and Computer Science (IMLCS2013)*, 9–13.
- Albanie, S.; Nagrani, A.; Vedaldi, A.; and Zisserman, A. 2018. Emotion recognition in speech using cross-modal transfer in the wild. In *Proceedings of the 26th ACM international conference on Multimedia*, 292–301.
- Arunnethru, J.; and Geetha, M. K. 2017. Automatic human emotion recognition in surveillance video. In *Intelligent Techniques in Signal Processing for Multimedia Security*, 321–342. Springer.
- Barrett, L. F.; Mesquita, B.; Ochsner, K. N.; and Gross, J. J. 2007. The experience of emotion. *Annu. Rev. Psychol.* 58: 373–403.
- Bhattacharya, U.; Mittal, T.; Chandra, R.; Randhavane, T.; Bera, A.; and Manocha, D. 2020. STEP: Spatial Temporal Graph Convolutional Networks for Emotion Perception from Gaits. In *AAAI*, 1342–1350.
- Chen, L.; Zhang, H.; Xiao, J.; Liu, W.; and Chang, S.-F. 2018. Zero-shot visual recognition using semantics-preserving adversarial embedding networks. In *Proceedings of the IEEE Conference on Computer Vision and Pattern Recognition*, 1043–1052.
- Cordaro, D. T.; Keltner, D.; Tshering, S.; Wangchuk, D.; and Flynn, L. M. 2016. The voice conveys emotion in ten globalized cultures and one remote village in Bhutan. *Emotion* 16(1): 117.
- Cowen, A.; Sauter, D.; Tracy, J. L.; and Keltner, D. 2019. Mapping the passions: Toward a high-dimensional taxonomy of emotional experience and expression. *Psychological Science in the Public Interest* 20(1): 69–90.
- Crenn, A.; Khan, R. A.; Meyer, A.; and Bouakaz, S. 2016. Body expression recognition from animated 3D skeleton. In *2016 International Conference on 3D Imaging (IC3D)*, 1–7. IEEE.
- De Silva, P. R.; Osano, M.; Marasinghe, A.; and Madurapperuma, A. P. 2006. Towards recognizing emotion with affective dimensions through body gestures. In *7th International Conference on Automatic Face and Gesture Recognition (FGRO6)*, 269–274. IEEE.
- Deng, J.; Xu, X.; Zhang, Z.; Frühholz, S.; and Schuller, B. 2017. Semisupervised autoencoders for speech emotion recognition. *IEEE/ACM Transactions on Audio, Speech, and Language Processing* 26(1): 31–43.
- Dinu, G.; Lazaridou, A.; and Baroni, M. 2014. Improving zero-shot learning by mitigating the hubness problem. *arXiv preprint arXiv:1412.6568*.
- Ekman, P.; and Friesen, W. V. 1967. Head and body cues in the judgment of emotion: A reformulation. *Perceptual and motor skills*.
- Ekman, P.; and Friesen, W. V. 2003. *Unmasking the face: A guide to recognizing emotions from facial clues*. Ishk.
- Gao, J.; Zhang, T.; and Xu, C. 2019. I know the relationships: Zero-shot action recognition via two-stream graph convolutional networks and knowledge graphs. In *Proceedings of the AAAI Conference on Artificial Intelligence*, volume 33, 8303–8311.
- Garcia-Ceja, E.; Riegler, M.; Kvernberg, A. K.; and Torresen, J. 2019. User-adaptive models for activity and emotion recognition using deep transfer learning and data augmentation. *User Modeling and User-Adapted Interaction* 1–29.
- Goodfellow, I.; Pouget-Abadie, J.; Mirza, M.; Xu, B.; Warde-Farley, D.; Ozair, S.; Courville, A.; and Bengio, Y. 2014. Generative adversarial nets. In *Advances in neural information processing systems*, 2672–2680.
- Grandjean, D.; Sander, D.; and Scherer, K. R. 2008. Conscious emotional experience emerges as a function of multilevel, appraisal-driven response synchronization. *Consciousness and cognition* 17(2): 484–495.
- Gunes, H.; and Piccardi, M. 2007. Bi-modal emotion recognition from expressive face and body gestures. *Journal of Network and Computer Applications* 30(4): 1334–1345.
- Holt, C. A.; and Roth, A. E. 2004. The Nash equilibrium: A perspective. *Proceedings of the National Academy of Sciences* 101(12): 3999–4002.
- Hossain, M. S.; and Muhammad, G. 2019. Emotion recognition using deep learning approach from audio–visual emotional big data. *Information Fusion* 49: 69–78.
- Hubert Tsai, Y.-H.; Huang, L.-K.; and Salakhutdinov, R. 2017. Learning robust visual-semantic embeddings. In *Proceedings of the IEEE International Conference on Computer Vision*, 3571–3580.
- Karg, M.; Kühnlenz, K.; and Buss, M. 2010. Recognition of affect based on gait patterns. *IEEE Transactions on Systems, Man, and Cybernetics, Part B (Cybernetics)* 40(4): 1050–1061.
- Kingma, D. P.; and Ba, J. 2014. Adam: A method for stochastic optimization. *arXiv preprint arXiv:1412.6980* URL <https://arxiv.org/pdf/1412.6980v9.pdf>.
- Liu, Z.; Wu, M.; Cao, W.; Chen, L.; Xu, J.; Zhang, R.; Zhou, M.; and Mao, J. 2017. A facial expression emotion recognition based human-robot interaction system.
- Long, Y.; Liu, L.; Shao, L.; Shen, F.; Ding, G.; and Han, J. 2017. From zero-shot learning to conventional supervised classification: Unseen visual data synthesis. In *Proceedings of the IEEE Conference on Computer Vision and Pattern Recognition*, 1627–1636.
- Makhzani, A.; Shlens, J.; Jaitly, N.; Goodfellow, I.; and Frey, B. 2015. Adversarial autoencoders. *arXiv preprint arXiv:1511.05644*.
- Mandal, D.; Narayan, S.; Dwivedi, S. K.; Gupta, V.; Ahmed, S.; Khan, F. S.; and Shao, L. 2019. Out-of-distribution detection for generalized zero-shot action recognition. In *Proceedings of the IEEE Conference on Computer Vision and Pattern Recognition*, 9985–9993.
- Meeren, H. K.; van Heijnsbergen, C. C.; and de Gelder, B. 2005. Rapid perceptual integration of facial expression and emotional body language. *Proceedings of the National Academy of Sciences* 102(45): 16518–16523.



- Michalak, J.; Troje, N. F.; Fischer, J.; Vollmar, P.; Heidenreich, T.; and Schulte, D. 2009. Embodiment of sadness and depression gait patterns associated with dysphoric mood. *Psychosomatic medicine* 71(5): 580–587.
- Mikolov, T.; Chen, K.; Corrado, G.; and Dean, J. 2013. Efficient estimation of word representations in vector space. *arXiv preprint arXiv:1301.3781*.
- Mishra, A.; Krishna Reddy, S.; Mittal, A.; and Murthy, H. A. 2018. A generative model for zero shot learning using conditional variational autoencoders. In *Proceedings of the IEEE Conference on Computer Vision and Pattern Recognition Workshops*, 2188–2196.
- Mittal, T.; Bhattacharya, U.; Chandra, R.; Bera, A.; and Manocha, D. 2020. M3ER: Multiplicative Multimodal Emotion Recognition using Facial, Textual, and Speech Cues. In *AAAI*, 1359–1367.
- Montepare, J. M.; Goldstein, S. B.; and Clausen, A. 1987. The identification of emotions from gait information. *Journal of Nonverbal Behavior* 11(1): 33–42.
- Qin, J.; Liu, L.; Shao, L.; Shen, F.; Ni, B.; Chen, J.; and Wang, Y. 2017. Zero-shot action recognition with error-correcting output codes. In *Proceedings of the IEEE Conference on Computer Vision and Pattern Recognition*, 2833–2842.
- Randhavane, T.; Bhattacharya, U.; Kapsaskis, K.; Gray, K.; Bera, A.; and Manocha, D. 2019. Identifying emotions from walking using affective and deep features. *arXiv preprint arXiv:1906.11884*.
- Robinson, M. D.; and Clore, G. L. 2002. Belief and feeling: evidence for an accessibility model of emotional self-report. *Psychological bulletin* 128(6): 934.
- Russell, J. A. 1980. A circumplex model of affect. *Journal of personality and social psychology* 39(6): 1161.
- Sanders, J. B.; Bremmer, M. A.; Comijs, H. C.; Deeg, D. J.; and Beekman, A. T. 2016. Gait speed and the natural course of depressive symptoms in late life; an independent association with chronicity? *Journal of the American Medical Directors Association* 17(4): 331–335.
- Sapiński, T.; Kamińska, D.; Pelikant, A.; and Anbarjafari, G. 2019. Emotion recognition from skeletal movements. *Entropy* 21(7): 646.
- Saragih, J. M.; Lucey, S.; and Cohn, J. F. 2009. Face alignment through subspace constrained mean-shifts. In *2009 IEEE 12th International Conference on Computer Vision*, 1034–1041. Ieee.
- Schonfeld, E.; Ebrahimi, S.; Sinha, S.; Darrell, T.; and Akata, Z. 2019. Generalized zero-and few-shot learning via aligned variational autoencoders. In *Proceedings of the IEEE Conference on Computer Vision and Pattern Recognition*, 8247–8255.
- Shi, Y.; Siddharth, N.; Paige, B.; and Torr, P. 2019. Variational mixture-of-experts autoencoders for multi-modal deep generative models. In *Advances in Neural Information Processing Systems*, 15718–15729.
- Tawari, A.; and Trivedi, M. M. 2010. Speech emotion analysis in noisy real-world environment. In *2010 20th International Conference on Pattern Recognition*, 4605–4608. IEEE.
- Volkova, E. P.; Mohler, B. J.; Dodds, T. J.; Tesch, J.; and Bülthoff, H. H. 2014. Emotion categorization of body expressions in narrative scenarios. *Frontiers in psychology* 5: 623.
- Wan, Z.; Chen, D.; Li, Y.; Yan, X.; Zhang, J.; Yu, Y.; and Liao, J. 2019. Transductive zero-shot learning with visual structure constraint. In *Advances in Neural Information Processing Systems*, 9972–9982.
- Wegrzyn, M.; Vogt, M.; Kireclioglu, B.; Schneider, J.; and Kissler, J. 2017. Mapping the emotional face. How individual face parts contribute to successful emotion recognition. *PloS one* 12(5): e0177239.
- Xian, Y.; Lorenz, T.; Schiele, B.; and Akata, Z. 2018. Feature generating networks for zero-shot learning. In *Proceedings of the IEEE conference on computer vision and pattern recognition*, 5542–5551.
- Yan, S.; Xiong, Y.; and Lin, D. 2018. Spatial temporal graph convolutional networks for skeleton-based action recognition. In *Thirty-second AAAI conference on artificial intelligence*.
- Yates, H.; Chamberlain, B.; Norman, G.; and Hsu, W. H. 2017. Arousal detection for biometric data in built environments using machine learning. In *IJCAI 2017 Workshop on Artificial Intelligence in Affective Computing*, 58–72.
- Zhao, M.; Adib, F.; and Katabi, D. 2016. Emotion recognition using wireless signals. In *Proceedings of the 22nd Annual International Conference on Mobile Computing and Networking*, 95–108.
- Zhou, D.; Zhang, X.; Zhou, Y.; Zhao, Q.; and Geng, X. 2016. Emotion distribution learning from texts. In *Proceedings of the 2016 Conference on Empirical Methods in Natural Language Processing*, 638–647.
- Zhu, Y.; Elhoseiny, M.; Liu, B.; Peng, X.; and Elgammal, A. 2018. A generative adversarial approach for zero-shot learning from noisy texts. In *Proceedings of the IEEE conference on computer vision and pattern recognition*, 1004–1013.